THINK INDIA JOURNAL

ISSN: 0971-1260
Vol-22-Issue-17-September-2019

Investigation of Mechanical Strength and Material Characterization Ondisparate TIG-Welded Joints of Ferrous Alloys

AkashGupta[a*], Prashant Kumar Singh[b], UpinderKumar[a], VishaldeepSingh[a]

aAssistant Professor, School of Mechanical Engineering, Lovely Professional University, Phagwara, Punjab, India-144411

b Technical Director, Mech Projects, Agra, Uttar Pradesh, India - 282007

Email: akash.19350@lpu.co.in

Abstract- In this experiment, TIG welding parameters influence on weld-ability of both stainless steel 304 and mild steel 1018 specimens with a dimension of 150 mm long x 75 mm wide x 3 mm thick is investigated. This paper investigated the microstructure and mechanical properties of dissimilar materials such as SS and MS joints by tungsten inert gas (TIG) welding. Fusion welding techniques are extensivelyadopted for joining ferrous and non-ferrous alloys.Performance of Tungsten inert gas (TIG) welding on between stainless steel 304 and Mild steel 1018 plate has been studied by optical microscope. The work objectives were the joining of dissimilar steel alloys was done by TIG welding with the innumerableinput variable like voltage, welding speed, and gas flow rate. The flux material of grade ER309 employed for the joining of these,unlike metals. Material characterization was carried out across the weldment region using an optical microscope. Mechanical properties like toughness, hardness were studied were done on dissimilar materials and check for their mechanical properties. Mechanical properties of the joints were evaluated by tensile tests and hardness tests. Taguchi L-9 technique has been used to analyze the data from experiments. An Orthogonal exhibit, S-N proportion, and ANOVA are utilized to examine the consequences of unlike joint and enhance the welding parameters. At long last, the adaptations tests have been done to contrast the anticipated qualities and the test esteems to affirm its viability in the strength analysis.

Index Terms-TIG welding, Microstructure, Tensile strength, Hardness, Taguchi method (TM),analysis of variance (ANOVA) orthogonal array, S/N ratio.

1 INTRODUCTION

In the fabrication, process equipment's made from stainless steel and mild steel are extensively adopted material from mechanical properties point of view.Arc fusing utilizing protecting gas is frequently utilized. Tungsten based gas welding is one of the most utilized welding techniques using inert gas as a medium to weld the material in a shielding zone[1].Welding of unlike metal

ISSN: 0971-1260
Vol-22-Issue-17-September-2019

is often used and the joint is mostly used where high strength or performance is required. For example, steel alloys components are most commonly used due to the benefit of high-temperature withstand capability in power generating devices. Beneath a specific temperature and weight, Moreover, the performance of low carbon alloy observed was satisfactory, So switching the other material in place of stainless steel faces major challenges in terms of financial effect. Most stainless steels can be effectively welded to low-alloy and low-carbon steels. The base metal of distinct material hasa different thermal coefficient in temperedsteel alloys and mild steel [2].

Tungsten Inert Gas (TIG) is most commonly used in fabrication industries for joining carbon-based and non-carbon based materialand broadly used in modern industry due to good weld bead surface finish obtained as shown in figure 1. This process offers numerousbenefits like fusion of unlike material, lessHAZ, no slag formation, etc. The weld quality is intenselyconsidered by weld bead dimensions. A high penetration to width ratio means a narrow weld. This also means a good quality of the weld [3].TIG welding can be done usually all orientations of variable metal thickness from 1mm to 6mm is largely joined using TIG[4].During the TIG welding process, thermal cycles in the welding process cause the chemical and microstructural changes. These alterationsinfluence the mechanical and material characteristics of the weld joints. Mechanical properties such as tensile yield strength, rigidity are typically controlled by a cross-sectional microstructure[5].Figure 2 shows the illustration of the unalike welding plate arrangement with the plate dimensions.

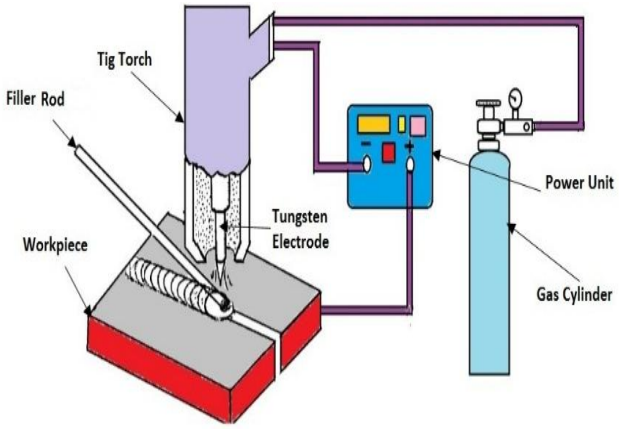

Figure 1 Schematic diagram of TIG welding process

ISSN: 0971-1260
Vol-22-Issue-17-September-2019

The materials adopted for dissimilar joining were SS-304 and MS-1018, nominally 3 mm in thickness. The chemical conformations of Specimen SS-304, MS-1018 and filler rod 309 are shown in Tables 1, 2 and 3, respectively.

Table 1 Chemical compositions of SS-304

%	C	Mn	S	P	Si	Ni	Cr	Cu
304	0.087	9.00	0.0009	0.055	0.23	1.050	15.45	1.64

Table 2 Chemical compositions of MS-1018

%	Fe	C	Mn	S	P
1018	98.97	0.17	0.68	0.051	0.040

Table 3 Chemical compositions of Filler Rod 309

%	C	Mg	Si	Mo	Ni	Cr
309	0.06	2.03	0.36	0.08	13.74	23.48

Prior to welding, the examples were arranged and welding should be possible. Transverse cross-areas were seen by optical microscopy (OM). The examples for optical microscopy were sliced opposite to the welding heading utilizing an electrical release machine. The Vickers hardness profile of the weld was estimated on the cross-area opposite to the welding heading. The elasticity is performed on a general testing machine (UTM)[6].

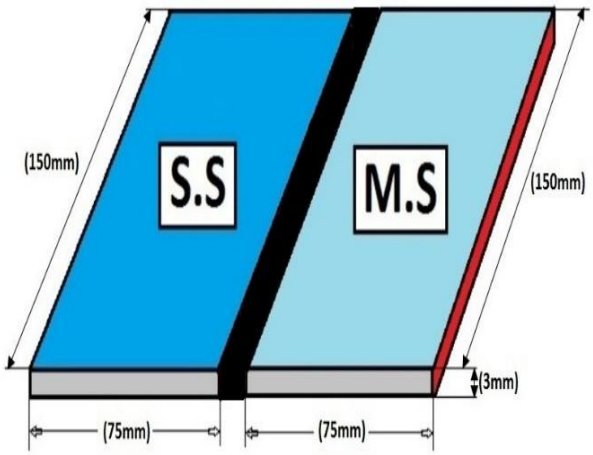

Figure 2 Illustration of the dissimilar plate arrangement for welding

ISSN: 0971-1260
Vol-22-Issue-17-September-2019

2 TAGUCHI METHOD

The Taguchi strategy is utilized to design the examinations. Taguchi system is the significance of considering efficiency utilizing the signal-noise ratio (S/N), bringing about the minimization of variable sets from variety because of wild parameters. The S/N proportion utilized for this sort of reaction taken as [7] [8].

- Smaller The Better n = -10 Log_{10}
- Higher The Better n = -10 Log_{10}
- Nominal the Best n = 10 Log_{10}

2.1 Taguchi L-9 Orthogonal Array

This approach was used to examine the effective parameter needs as per the desired mechanical properties. Procedure parameters in GTA Welding according using DOE in table 4 and table 5 respectively, nine examples were made by beat GTAW process which is appeared in the table [7].

Table 4. Standard Taguchi l-9 orthogonal array

Specimen No.	Welding Current	Gas Flow Rate	Welding Speed
A-1	1	1	1
B-1	1	1	2
C-1	1	1	3
D-1	2	2	2
E-1	2	2	3
F-1	2	2	1
G-1	3	3	3
H-1	3	3	1
I-1	3	3	2

Table 5 Sequence experiment was done by Taguchi method on the specimen

Specimen No.	Welding Current (amp)	Gas Flow Rate (l/min)	Welding Speed (mm/sec)
A-1	70	10	1.5
B-1	70	15	1.7
C-1	70	20	2.3

ISSN: 0971-1260
Vol-22-Issue-17-September-2019

D-1	80	10	1.7
E-1	80	15	2.3
F-1	80	20	1.5
G-1	90	10	2.3
H-1	90	15	1.5
I-1	90	20	1.7

3 WORK MATERIAL

Using dimensions of work-piece 75 mm long, 75 mm wide and 3 mm thick of different materials such as stainless steel and mild steel can be used for work material as shown in figure 3.

Figure 3 Diagram of TIG welding work material plates

TIG welding experiments are performed using the negative polarity [DCEN]. TIG welding using the process parameters are welding current (70, 80, 90) amp, Inert gas Flow Rate (10, 15, 20)Ltr./min &Feedrate (1.5, 1.7, 2.3)mm/sec. Constant parameters are Frequency 60Hz, Voltage 16V, Electrode diameter 1.6 & Electrode to work-piece distance 2mm.Table 6 shows the level of the selected parameter.

Table 6 Shows level and parameters

Levels	Welding Current	Gas Flow	Welding Speed

ISSN: 0971-1260
Vol-22-Issue-17-September-2019

		Rate	
Level-i	70	10	1.5
Level-ii	80	15	1.7
Level-iii	90	20	2.3

4 RESULTS AND DISCUSSION

4.1 Microstructure

Material characterization was done on all the welded samples near the weld zone and HAZ regionsfor each samplesusing a metallurgical microscope. The base metal microstructure has also been studied. Typical TIG welding microstructure was identified in all the welds with the help of a metallurgical microscope. All the welds produced by varying the process parameters were analyzed for microstructural appearance. Samples of size 15 mm x 15 mm at the joint interface were sectioned and mounted the samples such that the advancing side of the weld was always to the right. The mounted samples were prepared according to the standards given in metallography and microstructure. Metal has removed by filing to a depth of approximately 1 mm during the preparation of the specimen. Sandpaper of 220, 600, 1000, 1500 grits are used for cleaning to make the surface finished. Diamond paste has been used for finishing purposes to obtain as like mirror image surface. Alumina (Al2O3) was also used during cleaning the specimen on velvet paper which was mounted on the disc. After cleaning the specimen etching process has been used to obtain microstructure characteristics. The etchant used that having contained 5.0gm of picric acid, 5 ml of hydrochloric acid, and 100 ml of ethanol. In total 9 specimens have taken for the microstructure evolution in the welded region. All microstructure images have taken at 0.50μm or at 400x resolution. To the extent that the miniaturized scale structure of the base metal is concerned, unadulterated austenitic grains limits are seen in every one of the examples. One delegate base metal microstructure is shown in Figure 4.

ISSN: 0971-1260
Vol-22-Issue-17-September-2019

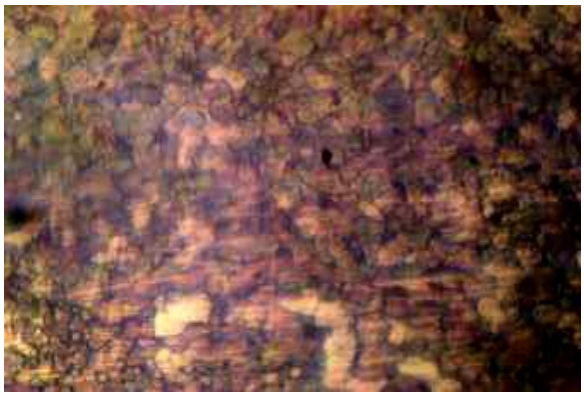

Figure 4 Metallographic view of base metal

Very little variety is seen among the weld metal microstructures of nine examples as found from microstructures that appeared in Figure 5. When all is said in done, austenitic grains are uncovered under the magnifying lens, in which precipitation of ferrite is additionally present. Nonetheless, grains are seen as coarser in weld metal than in base metal. This might be ascribed to the lower cooling rate in the weld area. In Figure 5, in the weld district, columnar grains of ferrite have been seen all through the structure. Austenite grains are prolonged, in Figure, a portion of the parts accelerated carbide has been found. In practically every one of the examples, hints of δ-ferrite are seen in HAZ under the magnifying instrument. Scattered carbide stages are found in the HAZ locale of test number B-1. This example shows the most minimal UTS in the pliable test. Be that as it may, no critical reason behind this has been found from a microstructural investigation of HAZ. On the off chance that weld metal microstructures of the considerable number of tests are contrasted and either base metal or HAZ microstructures, it is discovered that weld metal microstructure is appearing to be particularly unique from HAZ and base metalmicrostructures. In the majority of the examples, columnar-dendritic grain developments are seen in the weld microstructure. In sample number C-1, full austenitic structure with small or fine grain has been observed. This sample has shown the highest UTS. In general, more or less uniform distribution of austenite grains of equal size is seen throughout the structure, in which precipitation of carbide is revealed. In the weld-HAZ progress area, in certain examples, more measure of δ-ferrite is accelerated, in light of the fact that weakening less weld metal can't reach to the base metal. Along these lines, the base metal is immediately softened and hardened. As solidification time is less, δ-ferrite cannot get enough time for total transformation into the complete austenitic structure. Microstructures developed at different regions of the weld

ISSN: 0971-1260
Vol-22-Issue-17-September-2019

beads are dependent on the compositions of base and filler materials, dilution, heating and cooling cycles, and many other factors. A little bit of variation found in the microstructures among nine samples may be linked with the above factors, particularly with heating and cooling cycles. Varied parametric combinations during welding, influence heat input, heat input rate and cooling cycle. This, in turn, influences microstructures. This perspective might be considered in a broad way in future work.

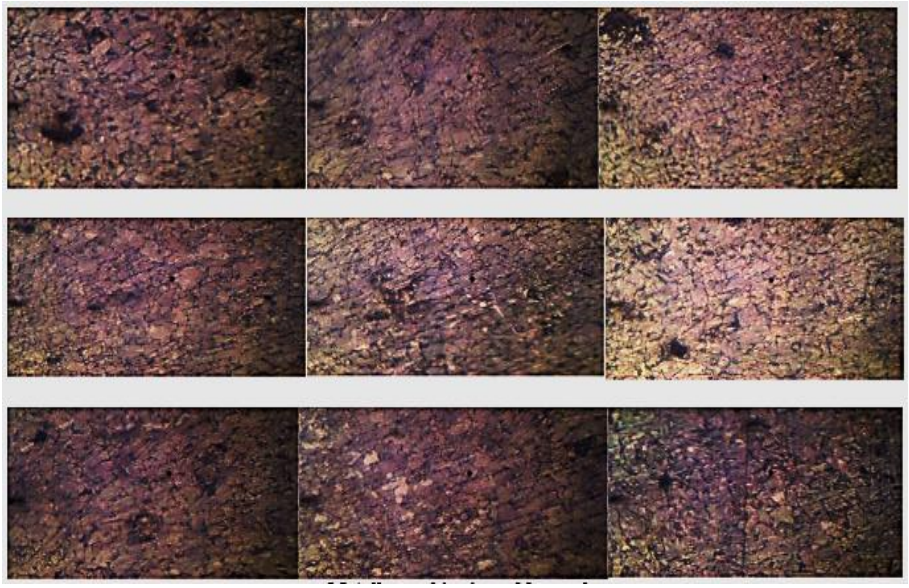

Figure 5 Metallographic view of 9 samples

4.2 Tensile Strength

Dog bone shaped tensile testing specimen was prepared using various cutting machines.Figure 6 shows the ready specimen as per the ASTM standards.

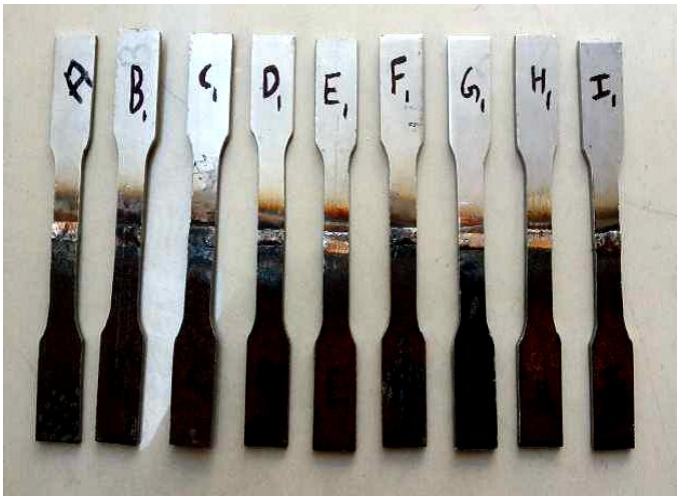

Figure 6 The tensile test specimens

ISSN: 0971-1260
Vol-22-Issue-17-September-2019

Tensile test specimens are checked on the UTM and picture perspective of test sample subsequent to testing as appeared in figure7.

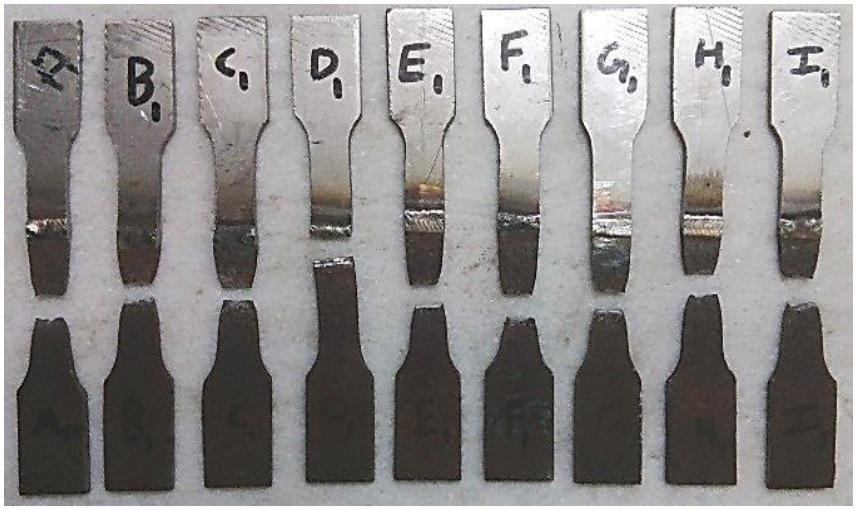

Figure 7 Photographic view of the tensile test specimen after testing

4.2.1 Consequencesof Tensile Test

The testing has been accomplished on a universal testing machine and explored significant tensile strength and corresponding strain of the welded tests. The consequences of tensile tests are given in Table 7. The ductile test outcomes show that for the greater part of the examples, rigidity is good. It is commonly desired that failure doesn't happen inside the weld area. From Table, it is discovered that under some parametric states of current, gas stream rate and welding speed, extreme rigidity is surprisingly great. For test numbers 1, 2, 3, 4, 5, 6, 7, 8, 9, it is inside the scope of 480 MPa – 520 MPa. For test number 3, extreme elasticity is greatest and for test number 2, extreme rigidity is least.

Table 7 Tensile test results

Ex. No.	Welding Current (Amp)	Gas Flow Rate (L/Min)	Welding Speed (mm/Sec)	Tensile Strength (N/mm^2)	S/N Ratio
A-1	70	10	1.5	511	27.08
B-1	70	15	1.7	480	26.81
C-1	70	20	2.3	520	27.16
D-1	80	10	1.7	493	26.92
E-1	80	15	2.3	498	26.97

ISSN: 0971-1260
Vol-22-Issue-17-September-2019

F-1	80	20	1.5	519	27.15
G-1	90	10	2.3	514	27.10
H-1	90	15	1.5	502	27.00
I-1	90	20	1.7	509	27.06

4.2.2 MainEffect of Tensile Strength

Based on the data in Table 4.1, the main effect plots for UTS have been obtained. From these plots, one can foresee the idea of the connection between UTS and information parameters. With an expansion in current, UTS increments. In this manner, the pattern is clear and definite. However, with an increase in both gas flow rate and welding speed, UTS first decreases and then increases beyond the 2nd level. Thus trends between i) gas flow rate and UTS and ii) welding speed and UTS are not consistent. Figure 8indicates that change in the levels of the inputvariable influences UTS. Factors like environmental conditions, some impurities present in the base metal may influence the process.

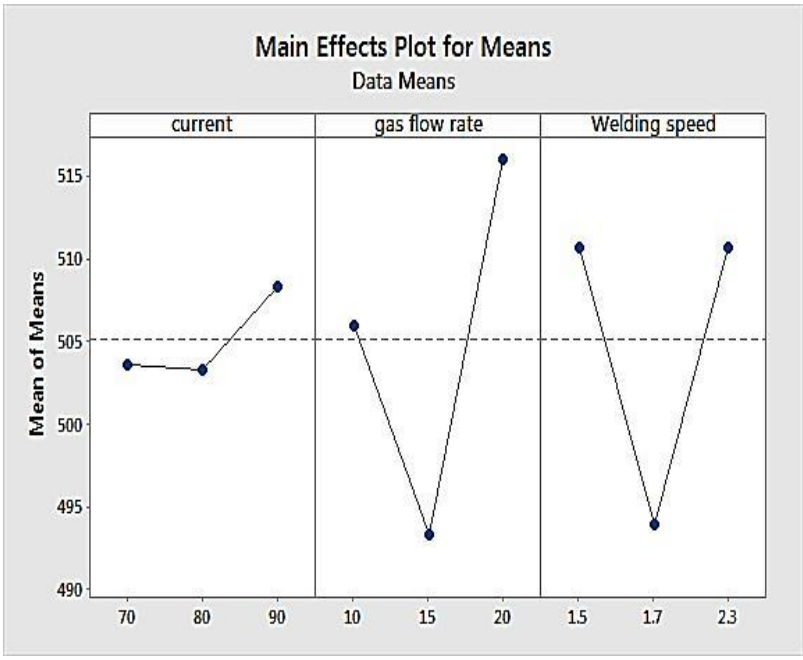

Figure 8 Main effect plots for the mean of UTS

4.2.3 ANOVA for Tensile Strength

Examination of change (ANOVA) utilizing MINITAB 17 programming has been executed to decide the commitment of procedure variable on elasticity for the Taguchi streamlining strategy. Table 8 shows the consequences of ANOVA for tensile stress. On the off chance that P-value is

ISSN: 0971-1260
Vol-22-Issue-17-September-2019

underneath 0.05, the conforming factor affects the reaction, at a 95% response. On inspecting the P-value, it is seen that the gas flow rate is the most noteworthy factor in light of the fact that the relating P-value is the least and it is underneath 0.05.

Table 8 The results of ANOVA for tensile strength

Source	DF	Adj SS	Adj MS	F-Value	P-Value
Regression	6	1376.67	229.444	108.68	0.009
Current	2	46.89	23.444	11.11	0.083
gas flow rate	2	774.22	387.111	183.37	0.005
Welding speed	2	555.56	277.778	131.58	0.008
Error	2	4.22	2.111		
Total	8	1380.89			
S	R-Sq		R-Sq(adj)		R-Sq(Pred)
1.45297	99.69%		98.78%		93.81%

Welding speed is likewise a huge factor since its worth is additionally under 0.05. Accordingly, the gas flow rate is the most noteworthy factor pursued by welding speed. Current is definitely not an extremely critical factor that impacts UTS. The predicted root squarefor this model was 99.69% which was most prominent than 80%. Itconcludesthat at any rate of 99.69% of the inconstancy in information for the reaction is clarified by approach. This shows the suggested model isagreeable.

CONCLUSIONS

In the existent work, butt welding of austenitic hardened steel of grade AISI 304 and mild steel of grade AISI 1018 has been joined using tungsten inert gas (TIG) welding, at altered degrees of current, welding speed and gas flow rate. The reactions considered are tensile stress and surface rigidity. In light of the aftereffects of the tests, demonstrating, and investigations made in the present examination, the accompanying ends are drawn.

- Unadulterated austenitic structure with a lot of austenitic twins is found in the microstructure of base metal. Very little variety is seen among the HAZ microstructures of nine examples. All in all, austenitic grains are uncovered under the magnifying lens, in which precipitation of ferrite is additionally present. Grains are seen as coarser in HAZ than in base metal. A

ISSN: 0971-1260
Vol-22-Issue-17-September-2019

limited quantity of δ-ferrite is seen in the microstructure of HAZ. In the majority of the examples, columnar-dendritic grain developments are seen in the weld microstructure.

- In single-target improvement by Taguchi, the goal is to augment elasticity independently for example independently. Taguchi S/N proportion idea was used and it was concludes that ideal circumstance for most extreme UTS was A3 B3 C1, for example, current = 90 A, gas flow rate = 20 liter/min, welding speed = 1.5mm/sec.

- Increase in current with increase the tensile strength of the material.

REFERENCES

[1]AhmetDurgutlu,"Experimentalinvestigation of the effect of hydrogen in argon as a shielding gas on TIG welding of austenitic stainless steel", Materials and Design,Vol. 25, pp 19–23, 2004.

[2] Cheng-HsienKuo,Kuang-Hung Tseng, Chang-Pin Chou, "Effect of activated TIG flux on the performance of dissimilar welds between mild steel and stainless steel",Key Engineering Materials, Vol. 479,pp 74-80, 2011.

[3] Vikesh, JagjitRandhawa, N M Suri, "Effect of a tig welding process parameters on penetration in mild steel plates", International Journal of Mechanical and Industrial Engineering, Vol3, Iss-2, pp 27-30, 2013.

[4] Dheeraj Singh,VedanshChaturvedi,JyotiVimal,**"**Parametric optimization of TIG process parameters using Taguchi and Grey Taguchi analysis", International Journal of Emerging Trends in Engineering and Development,Vol 4, issue 3, pp 64-78, 2013.

[5] Venkatasubramanian, G.,Sheik Mideen, A.,Abhay K Jha, "Microstructural characterization and corrosion behavior of top Surface of TIG-welded 2219−T87 Aluminium alloy", International Journal of Engineering Science and Technology, Vol. 5,No.03,2013.

[6] Prashant Kumar Singh, Pankaj Kumar, Baljeet Singh, Rahul Kumar Singh, "A review on TIG welding for optimizing process parameters on dissimilar joints", Int. Journal of Engineering Research and Application, Vol. 5, Issue 2, (Part -5), pp.125-128,2005.

ISSN: 0971-1260
Vol-22-Issue-17-September-2019

[7] Anoop C A,Pawan Kumar, "Application of Taguchi Methods and ANOVA in GTAW Process Parameters Optimization for Aluminium Alloy 7039", International Journal of Engineering and Innovative Technology, Volume 2, Issue 11,2013.

[8] J. Pasupathy, V.Ravisankar, "Parametric optimization of TIG welding parameters using taguchi method for dissimilar joint Low carbon steel with AA1050",International Journal of Scientific & Engineering Research, Volume 4,2013.